

Published in final edited form as:

Cancer Immunol Res. 2014 December ; 2(12): 1199–1208. doi:10.1158/2326-6066.CIR-14-0099.

STING contributes to anti-glioma immunity via triggering type-I IFN signals in the tumor microenvironment

Takayuki Ohkuri^{1,6,*}, Arundhati Ghosh^{4,8,*}, Akemi Kosaka^{1,6,*}, Jianzhong Zhu^{4,8}, Maki Ikeura⁶, Michael David⁹, Simon C. Watkins⁵, Saumendra N Sarkar^{3,4,8,†}, and Hideho Okada^{1,2,3,6,7,†}

¹Department of Neurological Surgery, University of Pittsburgh School of Medicine, Pittsburgh, PA 15213

²Department of Surgery, University of Pittsburgh School of Medicine, Pittsburgh, PA 15213

³Department of Immunology, University of Pittsburgh School of Medicine, Pittsburgh, PA 15213

⁴Department of Microbiology and Molecular Genetics, University of Pittsburgh School of Medicine, Pittsburgh, PA 15213

⁵Department of Cell Biology and Physiology, University of Pittsburgh School of Medicine, Pittsburgh, PA 15213

⁶Brain Tumor Program, University of Pittsburgh Cancer Institute, Pittsburgh, PA 15213, University of Pittsburgh Cancer Institute, Pittsburgh, PA 15213

⁷Cancer Immunology Program, University of Pittsburgh Cancer Institute, Pittsburgh, PA 15213, University of Pittsburgh Cancer Institute, Pittsburgh, PA 15213

⁸Cancer Virology Program, University of Pittsburgh Cancer Institute, Pittsburgh, PA 15213, University of Pittsburgh Cancer Institute, Pittsburgh, PA 15213

⁹Division of Biology, UCSD, La Jolla, CA 92093

Abstract

While type-I interferons (IFN) play critical roles in antiviral and antitumor activity, it remains to be elucidated how type-I IFNs are produced in sterile conditions of the tumor microenvironment and directly impacts tumor-infiltrating immune cells. Mouse *de novo* gliomas show increased expression of type-I IFN messages, and in mice, CD11b⁺ brain-infiltrating leukocytes (BIL) are the main source of type-I IFNs that are induced partially in a STING (stimulator of IFN genes)-dependent manner. Consequently, glioma-bearing *Sting*^{Gt/Gt} mice showed shorter survival, and lower expression levels of *Ifns* compared with wild-type mice. Furthermore, BILs of *Sting*^{Gt/Gt} mice show increased CD11b⁺ Gr-1⁺ immature myeloid suppressor and CD25⁺ Foxp3⁺ regulatory T (Treg) cells, and decreased IFN γ -producing CD8⁺ T cells. CD4⁺ and CD8⁺ T cells that received

[†]Corresponding Authors: Saumendra N. Sarkar, Ph.D., University of Pittsburgh Cancer Institute, Hillman Cancer Research Pavilion, Suite 1.8E, 5117 Centre Avenue, Building Pittsburgh, PA 15213, Phone: (412) 623-7720, Fax: (412) 623-7715, saumen@pitt.edu. Hideho Okada, MD, PhD, Department of Neurological Surgery, University of California San Francisco, Helen Diller Family Cancer Research, HD 472, 1450 3rd Street, San Francisco, CA 94158, OkadaH@neurosurg.ucsf.edu, Phone: (415) 476-1637.

*Contributed equally

Conflict of Interest: The authors declare no conflict of interests.

direct type-I IFN signals demonstrate lesser degrees of regulatory activity and increased levels of antitumor activity, respectively. Finally, intratumoral administration of a STING agonist (cyclic diguanylate monophosphate; c-di-GMP) improves the survival of glioma-bearing mice associated with enhanced type-I IFN signaling, *Cxcl10* and *Ccl5* and T-cell migration into the brain. In a combination with subcutaneous OVA peptide-vaccination, c-di-GMP increased OVA-specific cytotoxicity of BILs and prolonged the survival. These data demonstrate significant contributions of STING to antitumor immunity via enhancement of the type-I IFN signaling in the tumor microenvironment, and suggest a potential use of STING agonists for development of effective immunotherapy, such as the combination with antigen-specific vaccinations.

Introduction

Gliomas are the most common primary malignant brain tumors and carry a dismal prognosis despite current treatments, and new therapies are needed. Immunotherapies are promising in this regard. However, successful development of immunotherapy for gliomas requires detailed understanding of factors critical for anti-glioma immunity.

In addition to the ability of type-I IFNs to interfere with viral infection, they also enhance antitumor host immunity. Indeed, loss of type-I IFN signaling promotes tumorigenesis in a variety of tumor types, such as sarcomas (1), melanomas (2, 3), and in gliomas as we have reported (4). Although a growing body of evidence suggests that endogenously produced type-I IFNs participate in antitumor immune responses at the level of host hematopoietic cells (5, 6), the molecular mechanisms responsible for inducing the type-I IFN in the sterile tumor microenvironment remain elusive. Furthermore, impact of type-I IFN on immune cell populations participating in the antitumor response *in vivo* needs to be elucidated. In this regard, CD8 α ⁺ dendritic cells (DC) have been shown to require type-I IFNs for effective antitumor immunity (2, 3). Type-I IFNs directly enhance *in vivo* clonal expansion of CD4⁺ T cells following immunizations against lymphocytic choriomeningitis viruses, (7), promote the survival of CD8⁺ T cells, and stimulate the development of cytolytic functions including the production of IFN γ (8). Although we have previously demonstrated a critical role of type-I IFNs on maturation of glioma-infiltrating CD11c⁺ DCs (4), it still remains to be elucidated how type-I IFNs are induced in the glioma microenvironment and whether they directly impact T-cell functions.

STING has recently been identified as one of the critical adaptors for cytosolic DNA sensing. It plays a critical role in host defense against viral and intracellular bacteria by regulating type-I IFN signaling and innate immunity (9–12). STING is stimulated downstream of DNA sensors, such as helicase DDX41 [DEXD/H-box helicases 41] (13), and cyclic dinucleotides (CDNs), such as c-di-GMP, c-di-AMP, cGMP-AMP (cGAMP), or 10-carboxymethyl-9-acridanone (CMA) (14–18), thereby leading production of type-I IFNs. STING-deficient mice or cells show increased susceptibility to infection by several microbes and diminished levels of type-I IFNs in response to several microbes and CDNs (19).

Considering that there are abundant dying tumor cells that release their genomic (g)DNA in the tumor microenvironment (20), we evaluated our hypothesis that STING-mediated DNA sensing is involved in type-I IFN production in the glioma microenvironment, and

stimulation of STING with its agonist enhances anti-glioma immunity including T-cell responses.

Materials and Methods

Mice

Wild type (WT) C57BL/6 (H-2K^b) and C57BL/6-background *Sting*^{Gt/Gt} mice [C57BL/6J-*Tmem173*^{8t}] were purchased from The Jackson Laboratory. B6.129(Cg)-Gt(ROSA)26Sor^{tm4}(ACTB-tdTomato,-EGFP)Luo/J mice (“tdTomato” mice) were generated by breeding B6.Cg-Tg(Mx1-cre)1Cgn/J mice with B6.129(Cg)-Gt(ROSA)26Sor^{tm4}(ACTB-tdTomato,-EGFP)Luo/J mice (21). All mice were maintained and handled in accordance with the Animal Facility at the University of Pittsburgh per an Institutional Animal Care and Use Committee-approved protocol.

Antibodies and the synthetic peptide

The following monoclonal antibodies (mAb) were obtained from BD Biosciences (San Jose): anti-CD11c (HL3), anti-CD11b (M1/70), anti-Gr-1 (RB6-8C5). The following mAbs were obtained from eBioscience (San Diego): anti-CD4 (GK1.5), and anti-CD8 (53-6.7), anti-CD3 (145-2C11), anti-CD19 (eBio1D3), anti-IFN γ (XMG1.2), anti-CD25 (7D4), and anti-FoxP3 (NRRF-30). The H-2K^b-binding OVA₂₅₇₋₂₆₄ (SIINFEKL) peptide was synthesized in the University of Pittsburgh Peptide Synthesis Facility. For western blotting ISG54-specific polyclonal antibody (22) and actin-specific mAbs (Sigma-Aldrich) were used. For positive control, WT macrophages treated with 25 μ g/ml of polyI:C (for 48 h) were used.

De novo glioma induction

The procedure for intracerebroventricular DNA injection has been described previously (23). Briefly, the following DNA plasmids were mixed with *in vivo* compatible DNA transfection reagent, In vivo-JetPEI (Polyplus Transfection): pT2/C-Luc//PGK-SB100 (0.06 μ g/mouse), Sleeping beauty transposon (SB)-flanked pT2/CAG-NRasV12 (0.12 μ g/mouse), and pT2/shp53/mPDGF (0.12 μ g/mouse), and injected into the right lateral ventricle of neonate. Intracranial injection of glioma cell lines has been described previously (24).

Two-photon excitation microscopy

The procedure has been described previously (24).

In vivo bioluminescent intensity (BLI) measurement

The procedure has been described previously (24). Luciferin was obtained from Caliper Life Sciences.

Tumor cell culture

The GL261 mouse glioma cell line was kindly provided by Dr. Robert Prins (University of California-Los Angeles). The GL261-luc cell line was generated by transfection of GL261 cells (24) with a plasmid vector pcDNA3.1 encoding *luciferase* cDNA, followed by

selection with G418 (Sigma), limiting dilution and selection of a clone based on the highest luciferase expression level using luminometer in the presence of luciferin in culture. Survival of syngeneic mice bearing GL261-luc cells was confirmed to be comparable to those bearing parental GL261 cells (not shown). The Quad-GL261 cell line, kindly provided by Dr. John R. Ohlfest (University of Minnesota), expresses OVA₂₅₇₋₂₆₄, OVA₃₂₃₋₃₃₉, human gp100₂₅₋₃₃, and mouse I-E α ₅₂₋₆₈ (25). Stable expression of transgenes was maintained by G418 in the culture, and monitored every 3 months by evaluating their susceptibility against antigen-specific cytotoxic T-lymphocytes, such as Pmel-1 cells, which were derived from B6.Cg-*Thy1a*/Cy Tg(TcrRcrb)8Rest/J mice (The Jackson Laboratory). The RMA-S mouse thymoma cell line was kindly provided by Dr. Walter J. Storkus (University of Pittsburgh). All cell lines were tested to be mycoplasma-free. No other authentication assay was performed.

Quantitative real-time PCR (qRT-PCR)

Primers and probes for the following genes were obtained from Applied Biosystems: *Ifna6* (Mm01703458_s1), *Ifnb1* (Mm00439552_s1), *Foxp3* (Mm00475162_m1), *Tgfb1* (Mm01178820_m1), *Tbx21* (Mm00450960_m1), *Ifng* (Mm01168134_m1), *Ccl5* (Mm01302427_m1), *Cxcl10* (Mm00445235_m1) and *Gapdh* (Mm99999915_g1). In some experiments, following primers were used: mouse pan *Ifna* forward: CCTGAGAAGAGAAGAACACAGCC, reverse: GGCTCTCCAGACTTTCTGCTCTG; mouse pan *Ifnb* forward: CCGAGCA GAGATCTTCAGGAA; reverse: CCTGCAACCACCACTCATTCT; mouse *Gapdh* forward: TCACCACCATGGAGAAGGC, reverse: GCTAAGCAGTTGGTGGTGCA. *Gapdh* was used as an internal control. Relative expression levels compared with control samples were calculated in each experiment using the Ct method.

Stimulation of CD11b⁺ cells with gDNA in vitro

gDNA was isolated from GL261 and NIH 3T3 cell lines using Wizard[®] Genomic DNA purification kit from Promega. The final gDNA suspension was made in TE buffer (10 mM Tris.Cl, 1 mM EDTA). Aliquots of CD11b⁺ bone marrow-derived macrophage cells (5×10^5 cells/ml) from WT or *Sting*^{Gt/Gt} mice were stimulated with gDNA (1 or 5 μ g/ml). At 48 h, cells were harvested and total RNA was extracted. qRT-PCR analyses were performed with SsoFast[™] EvaGreen[®] Supermix (BIORAD) and data were analyzed with CFX manager 2.0 software from BIORAD.

BIL isolation and Flow cytometry

These procedures have been described previously (24).

Suppression assay

GFP-positive or -negative CD4⁺ T-cells derived from draining lymph nodes (LN) of glioma-bearing tdTomato mice were sorted by MoFlo Astros[™] (Beckman Coulter). CD8⁺ T cells were isolated from non-glioma-bearing WT mice and labeled with carboxyfluorescein succinimidyl ester (CFSE; life technologies) for 10 min in the incubator. After washing with medium, CD8⁺ T cells were co-cultured with GFP-negative or -positive CD4⁺ T cells in the

presence of Dynabeads (gibco by life technologies). After 60-hour incubation, samples were evaluated by BD Accuri™ C6.

Cytotoxicity assay

OVA-specific cytotoxicity of BILs was measured by 4 h ⁵¹Cr-release assay as described previously (4, 24). Briefly, freshly isolated BILs were incubated with ⁵¹Cr-labeled GL261 cells loaded with or without OVA₂₅₇₋₂₆₄ peptide (10µg/ml) for 4 h. For reverse antibody-dependent cell-mediated cytotoxicity (ADCC) of lymphocytes, GFP-positive or negative CD8⁺ T cells derived from draining LNs of glioma-bearing mice were sorted by MoFlo Astrios™ (Beckman Coulter), then incubated with ⁵¹Cr-labeled Fc-receptor-positive RMA-S cells pretreated with or without anti-CD3 mAb (10µg/ml, 145-2C11) (BD PharMingen) for 4 h. Percentage of cytotoxicity was calculated as described previously (26).

Treatment with c-di-GMP and vaccination with the OVA peptide in glioma-bearing mice

C-di-GMP (InvivoGen) was dissolved in physiologic water per manufacturer's instruction. Mice bearing gliomas received intracranial injections of either c-di-GMP (4µg/2µL/dose) or mock-treatment with solvent alone. Some mice received subcutaneous vaccinations with OVA₂₅₇₋₂₆₄ peptide (100µg/dose) emulsified in incomplete Freund Adjuvant (Difco Laboratories) on the same day as the c-di-GMP treatment.

Statistical analyses

The statistical significance of differences between two groups was determined by Student's t test; one-way ANOVA with Holm's post hoc test was conducted for multiple group comparisons. Log-rank test was used to determine statistically significant differences in survival curves among groups. All mouse data were analyzed by R Environment version 2.10.1.

Results

Induction of type-I IFN messages in mouse and gliomas

We first evaluated type-I IFN mRNA levels in mouse glioma microenvironment by qRT-PCR. Murine brain hemispheres bearing *de novo* glioma expressed significantly higher levels of *Ifna6*, *Ifna8* and *Ifnb1* compared with non-tumor-bearing contralateral hemispheres (Figure 1).

Type-I IFNs directly signal in Tcells in mice that are developing glioma

To determine the effects of type-I IFN expression in the glioma microenvironment, we utilized a novel reporter mouse model, in which the type-I IFN signaling induces the *Mx1* (IFN-induced GTP-binding protein) promoter-driven Cre recombinase, which turns the expression of *loxP*-flanked *tdTomato* off, and turns *GFP* expression on, thereby enabling us to monitor the induction of IFN signaling in the glioma microenvironment. Under two-photon microscopy, glioma tissues demonstrated higher levels of GFP signals compared with the normal (non-glioma-bearing) brain (Figure 2A), further substantiating IFN induction in the glioma microenvironment. Using flow cytometry, we evaluated the

percentage of GFP⁺ cells, in which IFN signaling has turned GFP signal on. In each of CD11b⁺ Gr-1⁺, CD11b⁺ CD11c⁺, CD19⁺ and CD3⁺ BIL subpopulations, glioma-bearing brains demonstrated a higher percentage of GFP⁺ cells compared with the spleen or inguinal lymph nodes (iLN)(Figure 2B and C). GFP⁺ RFP⁺ double-positive cells are thought to be the ones that have been exposed to IFN but still retain residual RFP protein. Since non-glioma-bearing brains do not contain sufficient numbers of BILs, we were unable to evaluate them. Nonetheless, the spleen and iLNs derived from non-glioma-bearing mice demonstrated similar percentages of GFP⁺ cells as those derived from glioma-bearing mice (**data not shown**), suggesting that type-I IFNs produced locally in the glioma tissue transmit their signals in BILs, but do not have significant impacts on cells in the spleen or iLN.

Type-I IFNs directly impact T-cell functions in mice that are developing glioma

We and others have previously demonstrated a critical role of the type-I IFN pathway in the function of tumor-infiltrating CD11c⁺ DCs as antigen-presenting cells (2–4). However, whether local production of type-I IFNs directly impacts the T cells in the glioma-bearing mice remains to be elucidated. The tdTomato mouse model allowed us to address this question *in vivo* during glioma progression. We sorted CD4⁺ and CD8⁺ T-cell populations from draining LNs based on their GFP expression. CD4⁺ T cells that received the type-I IFN signal (GFP⁺ cells) expressed significantly lower levels of *Foxp3* and *Tgfb1* compared with CD4⁺ T cells that did not receive the type-I IFN signal (GFP⁻ cells) (Figure 3A), suggesting that the GFP⁻ population contains more Treg cells. Indeed, GFP⁻ cells inhibited CD8⁺ T-cell proliferation more profoundly than GFP⁺ cells in the co-culture assay (Figure 3B). Among the CD8⁺ T cells, GFP⁺ cells expressed significantly higher levels of *Tbx21* and *Ifn γ* (Figure 3C), suggesting that the type-I IFN signal skews CD8⁺ cells towards type-I effector cells. Accordingly, GFP⁺ CD8⁺ cells demonstrated a higher cytotoxic activity than GFP⁻ cells (Figure 3D). Taken together, these results indicate that the type-I IFN signaling directly enhances antitumor activity of T cells in glioma-bearing mice.

CD11b⁺ cells express higher levels of *type-I Ifn* than CD11c⁺ cells in an STING-dependent manner

Next we focused on identifying the specific cells that are primarily responsible for producing IFN in glioma, so that we can define the signaling mechanism of IFN induction in the ‘sterile’ tumor microenvironment. As it was previously reported that CD11b⁺ and CD11c⁺ cells are responsible for IFN production (4), we isolated CD11b⁺ and CD11c⁺ cells from BILs derived from *SB*-glioma-bearing mice. As shown in Figure 4A, CD11b⁺ cells showed higher levels of *Ifna6* and *Ifnb1* expression than CD11c⁺ cells by qRT-PCR.

We next focused on the stimulus and the signaling pathway responsible for the observed *Ifn* induction. We excluded RNA sensors from our evaluation because, based on the literature (27), we thought it unlikely that high levels of immunostimulatory RNA, which can stimulate IFN production, are induced in the glioma microenvironment. While other receptors, such as High-mobility group protein B1 (28) and inflammasomes (29), have been implicated in antitumor immunity, these receptors do not directly cause strong IFN induction. We therefore hypothesized that gDNA derived from dying or dead cells can induce type-I IFNs through STING-mediated signaling in glioma-infiltrating macrophages

because both human and mouse glioma tissues contain necrotic areas that are heavily infiltrated by macrophages (23, 30). Indeed, we found up-regulation of *Sting* and *Ifi16*, which is involved in DNA virus sensing (31) (Supplementary Figure 1). Another DNA sensor *Aim2* that is responsible for inflammasome activation in response to DNA (32) was not up-regulated. We first tested this hypothesis *in vitro* by stimulating CD11b⁺ macrophages with gDNA derived from either GL261 glioma or NIH3T3 cells *in vitro*. We detected enhanced expression of pan *Ifna* and pan *Ifnb* at similar levels, which was abrogated by DNases (Figure 4B). The induction of pan *Ifna* was partially abrogated in STING-deficient cells (Figure 4C). These data indicate cell-derived gDNA, from either non-malignant or malignant cells, induce type-I IFNs at least partially in a STING-dependent manner, and led us to further investigate the role of STING in anti-glioma immunity.

STING contributes to anti-glioma immunity through production of type-I IFN in the glioma microenvironment

To determine the *in vivo* role of STING in glioma development, we induced *de novo* SB-gliomas in WT or *Sting*^{Gt/Gt} mice. Total RNA extracted from glioma-bearing brains of *Sting*^{Gt/Gt} mice showed significantly lower levels of *Ifna6* and *Ifnb1* compared with total RNA derived from WT mice (Figure 5A). Also, ISG54 protein, which is induced by type-I IFNs (22), was detected at a lower amount in the right (i.e., glioma-bearing) hemisphere of *Sting*^{Gt/Gt} mice than in the counterpart in WT mice (Figure 5B), indicating partial loss of IFN signaling. SB-glioma-bearing *Sting*^{Gt/Gt} mice exhibited significantly shorter survival compared with WT mice (Figure 5C). In BILs, *Sting*^{Gt/Gt} mice exhibited more CD11b⁺ Gr-1⁺ immature myeloid cells, which are likely myeloid-derived suppressor cells (MDSC) (33), and CD25⁺ Foxp3⁺ CD4⁺ Treg cells than WT mice. Furthermore, *Sting*^{Gt/Gt} mice had less IFN γ -producing CD8⁺ T-cells compared with WT mice (Figure 5D). These results suggest that STING is at least partially responsible for the spontaneous type-I IFN production, and impacts the phenotype of a variety of BIL populations, including T cells, in the glioma microenvironment. These data also led us to evaluate whether augmentation of the STING-mediated signal via administration of a STING agonist would enhance the anti-glioma immunity.

STING agonist enhances type-I IFN signaling and anti-glioma immunity

Among various ligands that have been reported to activate STING, structure-function studies have indicated that the cyclic dinucleotides have been the most authentic and robust activators of STING (34). When we administered c-di-GMP intratumorally in tdTomato mice bearing gliomas, BILs from c-di-GMP-treated mice demonstrated increased numbers of GFP⁺CD8⁺, GFP⁺CD4⁺ as well as GFP⁺CD11c⁺ cells compared with control mice treated with solvent alone (Figure S2). Treatment of glioma-bearing WT mice with c-di-GMP significantly prolonged survival (Figure 6A), and up-regulated *Ccl5* and *Cxcl10* levels compared with control treatment (Figure 6B) in a STING-dependent manner. In BILs, c-di-GMP treatment also enhanced tumor-homing of CD4⁺ and CD8⁺ T cells as well as IFN γ -producing CD8⁺ T cells in a STING-dependent manner (Figure 6C and D). In the *de novo* glioma model, administration of c-di-GMP also significantly inhibited glioma growth (Figure 6E). These data indicate that direct intratumoral administration of c-di-GMP

enhances anti-glioma immunity by enhancing the recruitment of T cells into the brain tumor site.

STING agonist enhances antitumor effects of peripheral vaccine

Finally, to evaluate whether c-di-GMP treatment would enhance the efficacy of vaccinations targeting a tumor-specific antigen, using the mouse Quad-GL261 glioma cell line expressing OVA₂₅₇₋₂₆₄ (25), we evaluated a combination of c-di-GMP and the OVA₂₅₇₋₂₆₄ peptide vaccine. While monotherapy with c-di-GMP alone significantly prolonged the survival of mice compared with vaccine alone or negative control with mock-treatment ($p < 0.01$), the combination treatment further enhanced the survival benefit with 7 of 10 mice surviving longer than 70 days ($p < 0.05$ compared with c-di-GMP alone; Figure 7A). All 10 mice treated with OVA₂₅₇₋₂₆₄ peptide vaccine alone died by day 47. In BIL analyses (Figure 7B), while c-di-GMP monotherapy significantly enhanced the tumor-homing of CD8⁺ T cells compared with mice receiving mock-treatment or vaccine alone, the combination regimen further enhanced the percentage of CD8⁺ cells compared with c-di-GMP alone. BILs obtained from mice receiving c-di-GMP monotherapy demonstrated a modest but significant cytotoxic activity against both OVA₂₅₇₋₂₆₄ peptide-pulsed and non-pulsed GL261 cells when compared with the control treatment, suggesting that c-di-GMP therapy induces cytotoxic responses against endogenous antigens in GL261 cells (Figure 7C). Furthermore, BILs obtained from mice receiving the combination therapy demonstrated a significantly higher OVA₂₅₇₋₂₆₄ peptide-specific cytotoxic activity compared with ones from mice receiving c-di-GMP alone, vaccine alone or mock-treatment (Figure 7C). These data strongly support the development of a combination strategy with vaccine and a STING agonist.

Discussion

This is, to our knowledge, the first study to describe the induction and roles of type-I IFNs in the glioma microenvironment. These mechanistic evaluations also led us to demonstrate the efficacy of c-di-GMP as an adjuvant in glioma immunotherapy.

Mouse glioma tissues spontaneously expressed type-I IFN mRNAs. Fuertes and colleagues have demonstrated that tumor-resident CD11c⁺ CD8 α ⁺ DCs are the source of type-I IFNs and these DCs are critical for induction of tumor-reactive T-cell responses (3). In human melanoma, Wenzel and colleagues have demonstrated a presence of strong type-I IFN signals in regressive melanocytic skin lesions (35). Our studies using tdTomato mice indicate that the type-I IFN signal in the glioma microenvironment indeed promotes type-I T-cell responses while inhibiting Tregs. On the other hand, development of gliomas in the brain did not impact immune cells in the spleen and iLNs, suggesting that spontaneous immune response in the glioma site does not induce systemic immune responses at least through the type-I IFN signals.

Based on our data with STING-deficient mice and cells, STING is at least partially responsible for the production of type-I IFNs responding to its ligands in the glioma microenvironment. Based on our data showing both glioma (i.e., GL261)- or non-transformed fibroblast (i.e., NIH3T3)-derived gDNA equally induced type-I IFN mRNAs in

myeloid cells in a STING-dependent manner, we postulate that gDNA released from either glioma or non-tumor stroma cells could be ligands for STING signaling. Indeed, necrosis is often observed in mouse *de novo* as well as human glioma lesions (q23, 30). It is likely that that STING is activated downstream of specific DNA sensors that are activated by gDNA, such as, *cyclic guanosine monophosphate-adenosine monophosphate (cGAMP) synthase (cGAS)* (36), *Ifi16*, *DDX41* (13, 15–18, 37) in the glioma tissue. cGAS may play a major role as cGAS produces cGAMP, which binds to and activates the adaptor protein STING, thereby inducing type I IFNs and other cytokines (36, 38). Further investigations are warranted to gain better understanding of STING activation in gliomas.

Cyclic-di-GMP had been demonstrated to be an effective vaccine adjuvant (39, 40) before it was found to be a ligand for STING in 2011 (16). Prior to our data in the current report, other groups have also demonstrated that the role of c-di-GMP as an effective adjuvant. Ebensen and colleagues have demonstrated that intranasal administrations of c-di-GMP in combination with vaccines induce significantly stronger humoral and cellular immune responses than the administration of the antigen alone (41). Moreover, Hu and colleagues have demonstrated that subcutaneous administrations of c-di-GMP plus *S. aureus*-associated antigens induce enhanced humoral immune responses in mice, leading prolonged survival after a challenge with cognate bacteria (42). These studies administered c-di-GMP three times to observe protective effects in their disease settings. On the other hand, in our glioma model, one c-di-GMP injection was sufficient to induce significant antitumor effects. This may be because our treatment was directed to the tumor site as local therapy, whereas systemic protection against infections requires systemic enhancement of the immune system. Interestingly, during the preparation of this manuscript, Miyabe and colleagues reported that subcutaneous administration of c-di-GMP delivered in liposome, but not c-di-GMP alone, can induce high-level IFN- β and antitumor immunity (43). It has also been demonstrated that intravenous administrations of c-di-GMP suppress vaccine-induced responses (44). Following the submission of our original manuscript, Chandra and colleagues have reported efficacy of intraperitoneally administered c-di-GMP in a metastatic 4T1 mammary adenocarcinoma model (45). As strategies to induce type-I IFNs, we (46, 47) and others (48–50) have conducted cancer immunotherapy clinical trials using TLR ligands. Based on our data in the current study, early phase clinical studies are warranted to evaluate the safety and efficacy of intratumoral administration of a STING agonist in patients with glioma.

Supplementary Material

Refer to Web version on PubMed Central for supplementary material.

Acknowledgments

The authors thank Drs. John R. Ohlfest, Adam J. Litterman (both at University of Minnesota) and Gary Kohanbash (University of Pittsburgh) for their technical and administrative assistance.

Grant Supports from: The NIH [2R01 NS055140, 2P01 NS40923, 1P01 CA132714, 5U24AI082673] and Musella Foundation for Brain Tumor Research and Information. This project used UPCI shared resources (Animal Facility, Small Animal Imaging facility, Cell and Tissue Imaging Facility, and Cytometry Facility) that are supported in part by NIH P30CA047904.

References

1. Schreiber RD, Old LJ, Smyth MJ. Cancer immunoediting: integrating immunity's roles in cancer suppression and promotion. *Science*. 2011; 331:1565–70. [PubMed: 21436444]
2. Diamond MS, Kinder M, Matsushita H, Mashayekhi M, Dunn GP, Archambault JM, et al. Type I interferon is selectively required by dendritic cells for immune rejection of tumors. *J Exp Med*. 2011; 208:1989–2003. [PubMed: 21930769]
3. Fuertes MB, Kacha AK, Kline J, Woo SR, Kranz DM, Murphy KM, et al. Host type I IFN signals are required for antitumor CD8+ T cell responses through CD8{alpha}+ dendritic cells. *J Exp Med*. 2011; 208:2005–16. [PubMed: 21930765]
4. Fujita M, Scheurer ME, Decker SA, McDonald HA, Kohanbash G, Kastenhuber ER, et al. Role of type I IFNs in antiglioma immunosurveillance--using mouse studies to guide examination of novel prognostic markers in humans. *Clin Cancer Res*. 2010; 16:3409–19. [PubMed: 20472682]
5. Dunn GP, Koebel CM, Schreiber RD. Interferons, immunity and cancer immunoediting. *Nat Rev Immunol*. 2006; 6:836–48. [PubMed: 17063185]
6. Swann JB, Hayakawa Y, Zerafa N, Sheehan KC, Scott B, Schreiber RD, et al. Type I IFN contributes to NK cell homeostasis, activation, and antitumor function. *J Immunol*. 2007; 178:7540–9. [PubMed: 17548588]
7. Havenar-Daughton C, Kolumam GA, Murali-Krishna K. Cutting Edge: The direct action of type I IFN on CD4 T cells is critical for sustaining clonal expansion in response to a viral but not a bacterial infection. *J Immunol*. 2006; 176:3315–9. [PubMed: 16517698]
8. Curtsinger JM, Valenzuela JO, Agarwal P, Lins D, Mescher MF. Type I IFNs provide a third signal to CD8 T cells to stimulate clonal expansion and differentiation. *J Immunol*. 2005; 174:4465–9. [PubMed: 15814665]
9. Xiao TS, Fitzgerald KA. The cGAS-STING pathway for DNA sensing. *Mol Cell*. 2013; 51:135–9. [PubMed: 23870141]
10. Fuertes MB, Woo SR, Burnett B, Fu YX, Gajewski TF. Type I interferon response and innate immune sensing of cancer. *Trends Immunol*. 2013; 34:67–73. [PubMed: 23122052]
11. Gajewski TF, Schreiber H, Fu YX. Innate and adaptive immune cells in the tumor microenvironment. *Nat Immunol*. 2013; 14:1014–22. [PubMed: 24048123]
12. Ishikawa H, Ma Z, Barber GN. STING regulates intracellular DNA-mediated, type I interferon-dependent innate immunity. *Nature*. 2009; 461:788–92. [PubMed: 19776740]
13. Zhang Z, Yuan B, Bao M, Lu N, Kim T, Liu YJ. The helicase DDX41 senses intracellular DNA mediated by the adaptor STING in dendritic cells. *Nat Immunol*. 2011; 12:959–65. [PubMed: 21892174]
14. Sun L, Wu J, Du F, Chen X, Chen ZJ. Cyclic GMP-AMP synthase is a cytosolic DNA sensor that activates the type I interferon pathway. *Science*. 2013; 339:786–91. [PubMed: 23258413]
15. Ablasser A, Schmid-Burgk JL, Hemmerling I, Horvath GL, Schmidt T, Latz E, et al. Cell intrinsic immunity spreads to bystander cells via the intercellular transfer of cGAMP. *Nature*. 2013; 503:530–4. [PubMed: 24077100]
16. Burdette DL, Monroe KM, Sotelo-Troha K, Iwig JS, Eckert B, Hyodo M, et al. STING is a direct innate immune sensor of cyclic di-GMP. *Nature*. 2011; 478:515–8. [PubMed: 21947006]
17. Cavlar T, Deimling T, Ablasser A, Hopfner KP, Hornung V. Species-specific detection of the antiviral small-molecule compound CMA by STING. *EMBO J*. 2013; 32:1440–50. [PubMed: 23604073]
18. Paludan SR, Bowie AG. Immune sensing of DNA. *Immunity*. 2013; 38:870–80. [PubMed: 23706668]
19. Ishikawa H, Barber GN. STING is an endoplasmic reticulum adaptor that facilitates innate immune signalling. *Nature*. 2008; 455:674–8. [PubMed: 18724357]
20. Schwarzenbach H, Hoon DS, Pantel K. Cell-free nucleic acids as biomarkers in cancer patients. *Nat Rev Cancer*. 2011; 11:426–37. [PubMed: 21562580]

21. Otero DC, Baker DP, David M. IRF7-dependent IFN-beta production in response to RANKL promotes medullary thymic epithelial cell development. *J Immunol.* 2013; 190:3289–98. [PubMed: 23440417]
22. Fensterl V, White CL, Yamashita M, Sen GC. Novel characteristics of the function and induction of murine p56 family proteins. *J Virol.* 2008; 82:11045–53. [PubMed: 18768971]
23. Wiesner SM, Decker SA, Larson JD, Ericson K, Forster C, Gallardo JL, et al. De novo induction of genetically engineered brain tumors in mice using plasmid DNA. *Cancer Res.* 2009; 69:431–9. [PubMed: 19147555]
24. Fujita M, Zhu X, Ueda R, Sasaki K, Kohanbash G, Kastenhuber ER, et al. Effective immunotherapy against murine gliomas using type 1 polarizing dendritic cells—significant roles of CXCL10. *Cancer Res.* 2009; 69:1587–95. [PubMed: 19190335]
25. Litterman AJ, Zellmer DM, Grinnen KL, Hunt MA, Dudek AZ, Salazar AM, et al. Profound impairment of adaptive immune responses by alkylating chemotherapy. *J Immunol.* 2013; 190:6259–68. [PubMed: 23686484]
26. Yanagita Y, Nishimura T, Gao XH, Mitomi T, Habu S. Natural cytotoxic T cells responsible for anti-CD3-induced cytotoxicity in mice. *Immunol Lett.* 1992; 31:137–42. [PubMed: 1531474]
27. Goubau D, Deddouch S, Reis e Sousa C. Cytosolic sensing of viruses. *Immunity.* 2013; 38:855–69. [PubMed: 23706667]
28. Apetoh L, Ghiringhelli F, Tesniere A, Obeid M, Ortiz C, Criollo A, et al. Toll-like receptor 4-dependent contribution of the immune system to anticancer chemotherapy and radiotherapy. *Nat Med.* 2007; 13:1050–9. [PubMed: 17704786]
29. Ghiringhelli F, Apetoh L, Tesniere A, Aymeric L, Ma Y, Ortiz C, et al. Activation of the NLRP3 inflammasome in dendritic cells induces IL-1beta-dependent adaptive immunity against tumors. *Nat Med.* 2009; 15:1170–8. [PubMed: 19767732]
30. Louis DN, Ohgaki H, Wiestler OD, Cavenee WK, Burger PC, Jouvet A, et al. The 2007 WHO classification of tumours of the central nervous system. *Acta Neuropathol (Berl).* 2007; 114:97–109. [PubMed: 17618441]
31. Unterholzner L, Keating SE, Baran M, Horan KA, Jensen SB, Sharma S, et al. IFI16 is an innate immune sensor for intracellular DNA. *Nat Immunol.* 2010; 11:997–1004. [PubMed: 20890285]
32. Hornung V, Ablasser A, Charrel-Dennis M, Bauernfeind F, Horvath G, Caffrey DR, et al. AIM2 recognizes cytosolic dsDNA and forms a caspase-1-activating inflammasome with ASC. *Nature.* 2009; 458:514–8. [PubMed: 19158675]
33. Ostrand-Rosenberg S, Sinha P, Beury DW, Clements VK. Cross-talk between myeloid-derived suppressor cells (MDSC), macrophages, and dendritic cells enhances tumor-induced immune suppression. *Semin Cancer Biol.* 2012; 22:275–81. [PubMed: 22313874]
34. Burdette DL, Vance RE. STING and the innate immune response to nucleic acids in the cytosol. *Nat Immunol.* 2013; 14:19–26. [PubMed: 23238760]
35. Wenzel J, Bekisch B, Uerlich M, Haller O, Bieber T, Tuting T. Type I interferon-associated recruitment of cytotoxic lymphocytes: a common mechanism in regressive melanocytic lesions. *Am J Clin Pathol.* 2005; 124:37–48. [PubMed: 15923172]
36. Gao D, Wu J, Wu YT, Du F, Aroh C, Yan N, et al. Cyclic GMP-AMP synthase is an innate immune sensor of HIV and other retroviruses. *Science.* 2013; 341:903–6. [PubMed: 23929945]
37. Bhat N, Fitzgerald KA. Recognition of cytosolic DNA by cGAS and other STING-dependent sensors. *Eur J Immunol.* 2014; 44:634–40. [PubMed: 24356864]
38. Schoggins JW, MacDuff DA, Imanaka N, Gainey MD, Shrestha B, Eitson JL, et al. Pan-viral specificity of IFN-induced genes reveals new roles for cGAS in innate immunity. *Nature.* 2014; 505:691–5. [PubMed: 24284630]
39. Chen W, Kuolee R, Yan H. The potential of 3',5'-cyclic diguanylic acid (c-di-GMP) as an effective vaccine adjuvant. *Vaccine.* 2010; 28:3080–5. [PubMed: 20197136]
40. Ebensen T, Libanova R, Schulze K, Yevsa T, Morr M, Guzman CA. Bis-(3',5')-cyclic dimeric adenosine monophosphate: strong Th1/Th2/Th17 promoting mucosal adjuvant. *Vaccine.* 2011; 29:5210–20. [PubMed: 21619907]

41. Ebensen T, Schulze K, Riese P, Morr M, Guzman CA. The bacterial second messenger c-diGMP exhibits promising activity as a mucosal adjuvant. *Clin Vaccine Immunol.* 2007; 14:952–8. [PubMed: 17567766]
42. Hu DL, Narita K, Hyodo M, Hayakawa Y, Nakane A, Karaolis DK. c-di-GMP as a vaccine adjuvant enhances protection against systemic methicillin-resistant *Staphylococcus aureus* (MRSA) infection. *Vaccine.* 2009; 27:4867–73. [PubMed: 19406185]
43. Miyabe H, Hyodo M, Nakamura T, Sato Y, Hayakawa Y, Harashima H. A new adjuvant delivery system 'cyclic di-GMP/YSK05 liposome' for cancer immunotherapy. *J Control Release.* 2014; 184C:20–7. [PubMed: 24727060]
44. Huang L, Li L, Lemos H, Chandler PR, Pacholczyk G, Baban B, et al. Cutting edge: DNA sensing via the STING adaptor in myeloid dendritic cells induces potent tolerogenic responses. *J Immunol.* 2013; 191:3509–13. [PubMed: 23986532]
45. Chandra D, Quispe-Tintaya W, Jahangir A, Asafu-Adjei D, Ramos I, Sintim HO, et al. STING ligand c-di-GMP improves cancer vaccination against metastatic breast cancer. *Cancer Immunol Res.* 2014; 2:901–10. [PubMed: 24913717]
46. Okada H, Kalinski P, Ueda R, Hoji A, Kohanbash G, Donegan TE, et al. Induction of CD8+ T-cell responses against novel glioma-associated antigen peptides and clinical activity by vaccinations with {alpha}-type 1 polarized dendritic cells and polyinosinic-polycytidylic acid stabilized by lysine and carboxymethylcellulose in patients with recurrent malignant glioma. *J Clin Oncol.* 2011; 29:330–6. [PubMed: 21149657]
47. Pollack IF, Jakacki RI, Butterfield LH, Okada H. Ependymomas: development of immunotherapeutic strategies. *Expert Rev Neurother.* 2013; 13:1089–98. [PubMed: 24117271]
48. Karbach J, Neumann A, Atmaca A, Wahle C, Brand K, von Boehmer L, et al. Efficient in vivo priming by vaccination with recombinant NY-ESO-1 protein and CpG in antigen naive prostate cancer patients. *Clin Cancer Res.* 2011; 17:861–70. [PubMed: 21163871]
49. Sabbatini P, Tsuji T, Ferran L, Ritter E, Sedrak C, Tuballes K, et al. Phase I trial of overlapping long peptides from a tumor self-antigen and poly-ICLC shows rapid induction of integrated immune response in ovarian cancer patients. *Clin Cancer Res.* 2012; 18:6497–508. [PubMed: 23032745]
50. Valmori D, Souleimanian NE, Tosello V, Bhardwaj N, Adams S, O'Neill D, et al. Vaccination with NY-ESO-1 protein and CpG in Montanide induces integrated antibody/Th1 responses and CD8 T cells through cross-priming. *Proc Natl Acad Sci U S A.* 2007; 104:8947–52. [PubMed: 17517626]

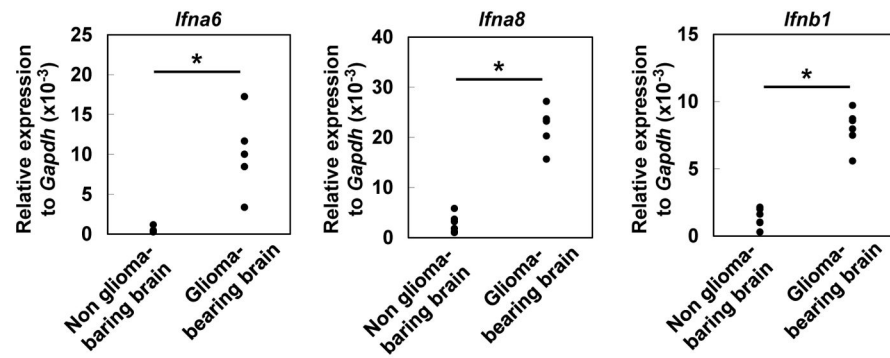


Figure 1. Type-I IFNs are detected in glioma tissues of mice

Mice bearing *SB*-induced glioma in the right hemisphere were sacrificed between days 40 to 50 (with tumors of similar size at $\sim 1 \times 10^7$ luciferase units). Total RNA was extracted from the left (non-glioma-bearing) and right (glioma-bearing) hemispheres of each brain separately (5 mice), and evaluated for expression of *Ifna6* (left), *Ifna8* (middle), and *Ifnb1* (right) by qRT-PCR. Each experiment was performed at least twice. * $p < 0.05$ based on Student's *t*-test.

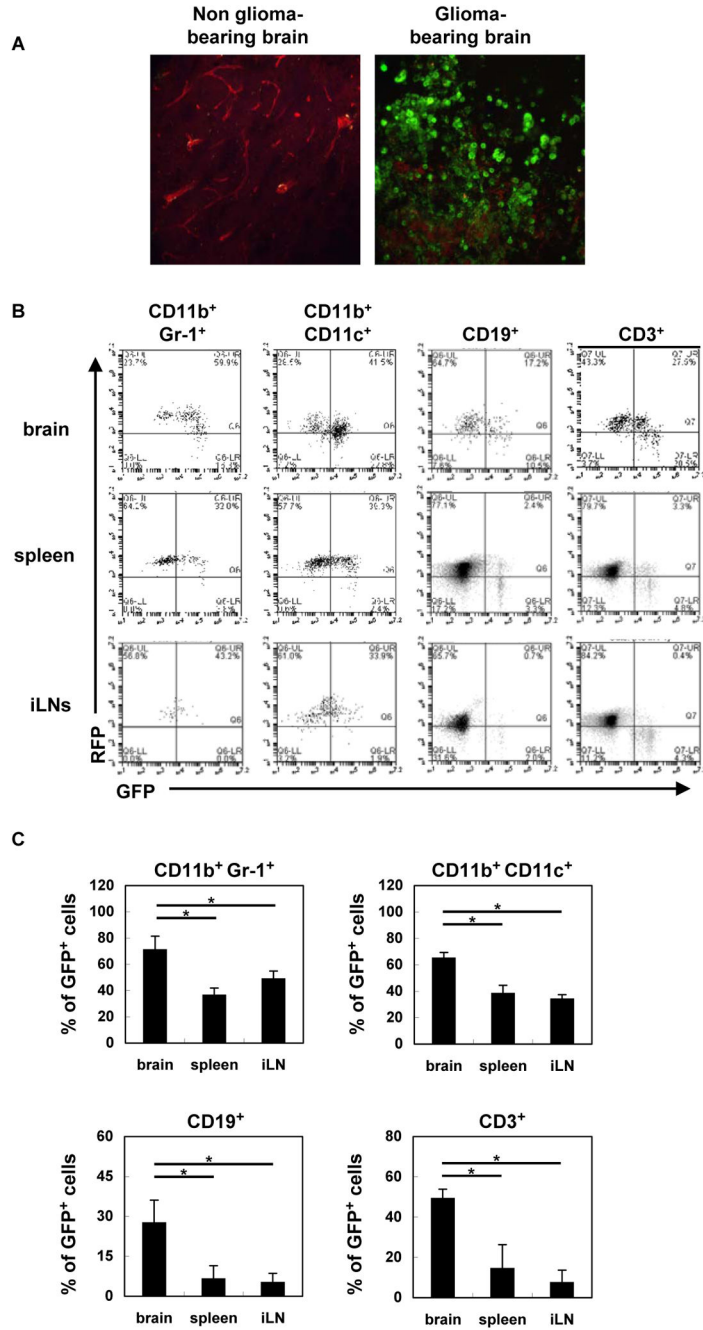


Figure 2. Type-I IFN signaling in the tumor microenvironment

tdTomato mice bearing *SB*-induced glioma were sacrificed between days 40 to 50. (A) Brain sections were evaluated by two-photon microscopy for GFP⁺ and RFP⁺ cells. Original magnification, 60 X. (B) BILs, splenocytes, and iLN cells were evaluated for the percentages of GFP⁺ cells. Representative flow histograms are shown. (C) Percentages of GFP⁺ cells in the glioma-bearing brain, spleen and inguinal LNs (3 mice/group). **p* < 0.05 based on Student's *t*-test.

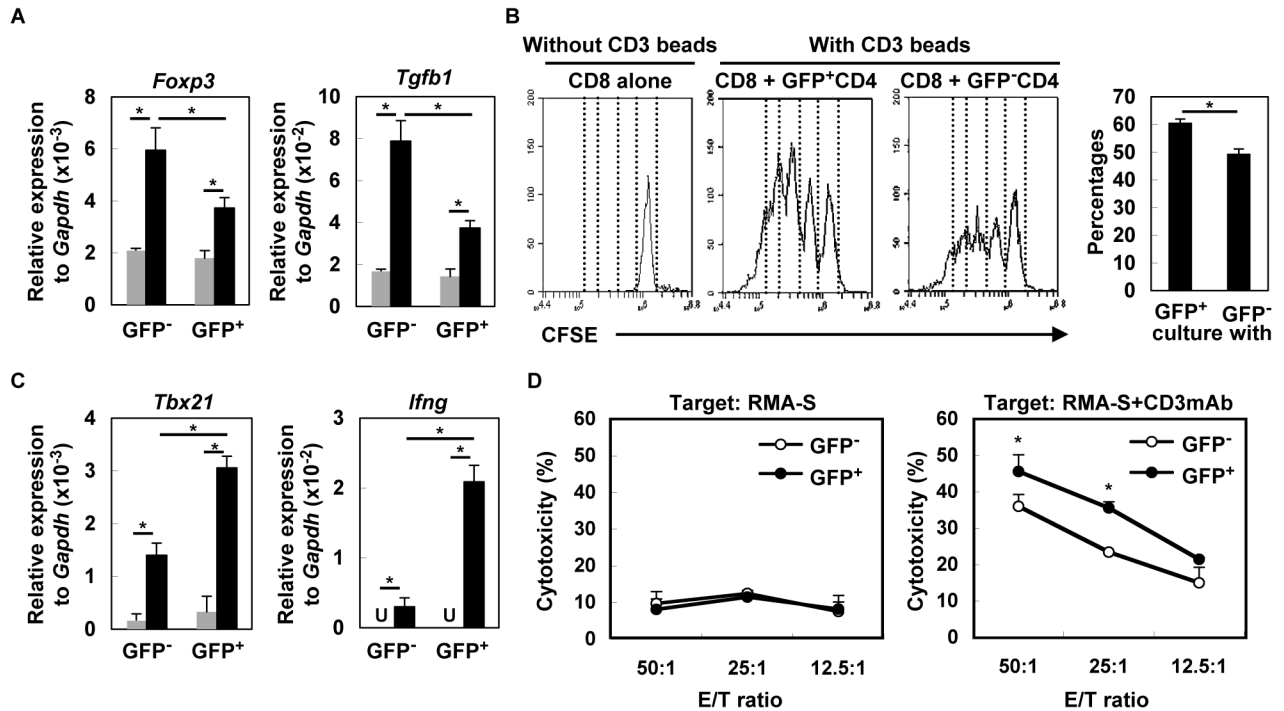


Figure 3. Type-I IFNs directly impact T-cell functions in glioma-developing mice

(A) CD4⁺ cells from draining LN derived from glioma-developing tdTomato mice were sorted into GFP⁻ or GFP⁺ cells and incubated with (black bars) or without (grey bars) anti-CD3mAb. After 4 h, total RNA was extracted for evaluation of *Foxp3* and *Tgfb1* mRNA levels by qRT-PCR. (B) CFSE-labeled WT CD8⁺ T-cells were co-cultured with GFP⁻ or GFP⁺ CD4⁺ T cells in the presence of CD3 beads. After 60 h, division of CFSE-labeled CD8⁺ T-cells gated by reactivity to PE-Cy7-conjugated anti-CD8mAb was evaluated by CFSE intensity. As a negative control, CFSE-labeled WT CD8⁺ T-cells were cultured without any stimulation (left panel). Histograms are representative of two independent experiments. The bar graph shows the percentage of CD8⁺ cells that have divided at least twice in each of two stimulation conditions (N=4/group; **p* < 0.05). (C) GFP⁻ or GFP⁺ CD8⁺ T-cells were incubated with (black bar) or without (grey bar) anti-CD3mAb. After 4 h, total RNA was extracted for evaluation of *Tbx21* and *Ifng* mRNA expression levels by qRT-PCR (U: undetected). (D) Cytotoxic activity of GFP⁻ and GFP⁺ CD8⁺ T cells was evaluated by ⁵¹Cr-release assay. RMA-S cells untreated (left panel) or pretreated (right panel) with anti-CD3mAb (10μg/mL) were used as target cells. Each experiment was performed at least twice. **p* < 0.05 compared at the same E/T ratio.

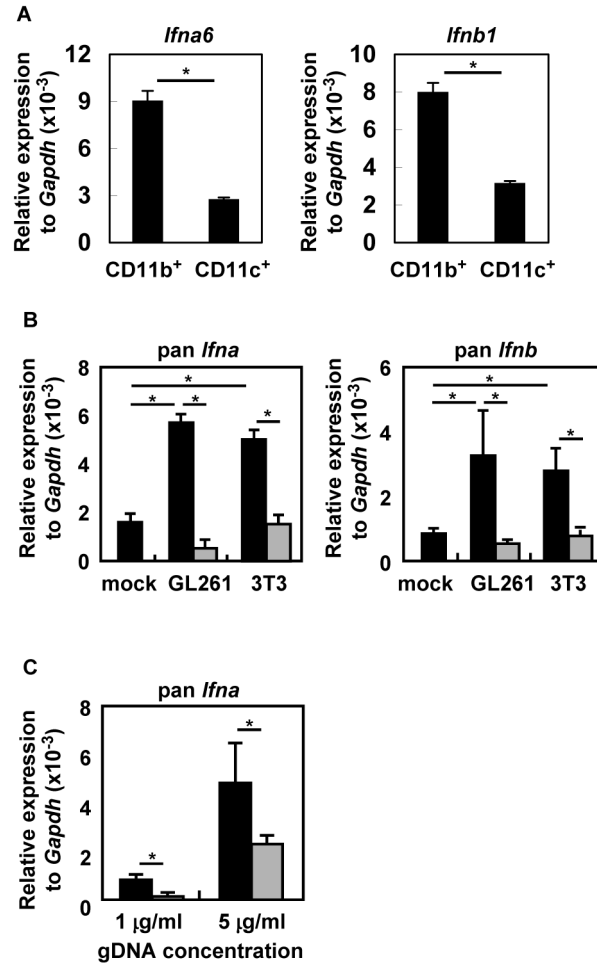


Figure 4. CD11b⁺ cells produce type-I IFNs in response to genomic DNA in a partially STING-dependent manner

(A) Total RNA was extracted from magnetic bead-enriched CD11b⁺ and CD11c⁺ BIL populations (purity was > 85% and > 80%, respectively) and evaluated for *Ifna6* and *Ifnb1* by qRT-PCR. (B) BMDM cells from WT mice were stimulated with gDNA derived from GL261 or NIH3T3 cell lines, or solvent only as mock treatment with (grey bars) or without (black bars) pre-treatment with DNase. After 48 h, total RNA was extracted and evaluated for pan *Ifna* and pan *Ifnb* by qRT-PCR. (C) BMDM from WT (black bars) or *Sting*^{Gt/Gt} (grey bars) mice were stimulated with GL261-derived gDNA (1 or 5 μ g/mL). After 48 h, total RNA was extracted and evaluated for pan *Ifna* by qRT-PCR. Each experiment was performed at least twice. * $p < 0.05$ based on Student's *t*-test.

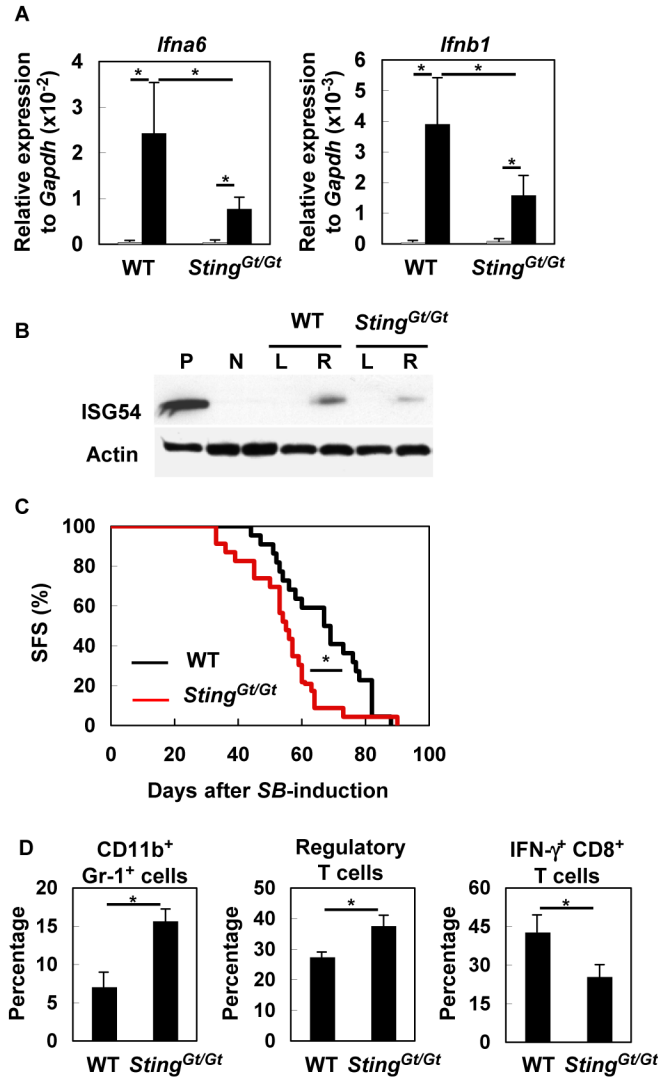


Figure 5. STING contributes to IFN production and anti-glioma immunity

(A) WT or *Sting*^{Gt/Gt} mice bearing *SB*-induced gliomas were sacrificed between days 40 to 50 (with tumors of similar size at $\sim 1 \times 10^7$ luciferase units). Total RNA was extracted from the left (non-tumor bearing; gray bars) and right (tumor-bearing; black bars) hemispheres of each brain separately (5–6 mice/group), and evaluated for expression of *Ifna6* (left) and *Ifnb1* (right) by qRT-PCR. * $p < 0.05$ based on Student's *t*-test. (B) Fifty μ g protein extracts were analyzed by SDS-PAGE and western blotting for detection of ISG54. "L" and "R" indicate samples from left and right hemispheres, respectively, of WT or *Sting*^{Gt/Gt} mice bearing *SB*-induced glioma. WT-derived macrophage sample treated with p(I): p(C) was used as positive control (P). Glioma-free WT mouse brain was used as negative control (N). Actin was used as an internal control. (C) Gliomas were induced in WT (22 mice; black line) or *Sting*^{Gt/Gt} mice (23 mice; red line) neonatal mice by the *SB*-transposon system. Survival was monitored. * $p < 0.05$ based on Log-rank test. (D) Percentages of CD11b⁺ Gr-1⁺, CD25⁺ Foxp3⁺ CD4⁺ (Treg), and IFN γ -producing CD8⁺ T BILs were compared

between the two groups by flow cytometry. Each experiment except for (C) was performed at least twice. * $p < 0.05$ based on Student's t -test.

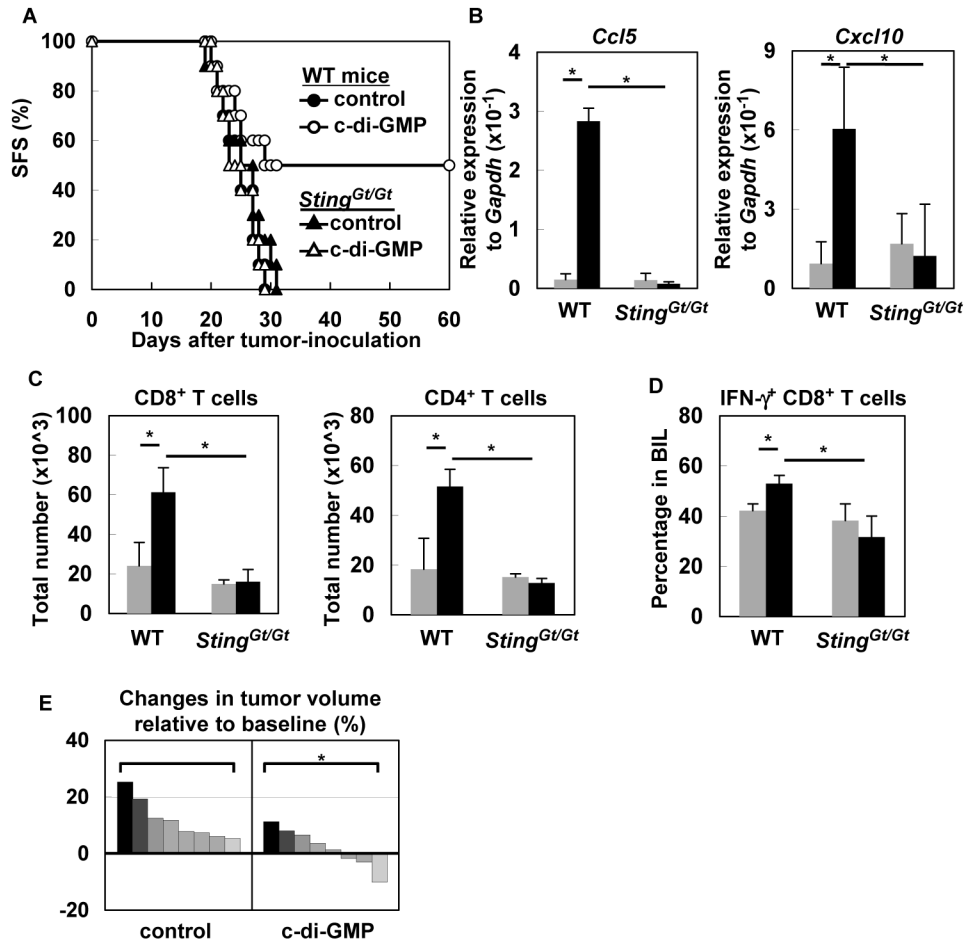


Figure 6. STING agonist enhances anti-glioma immunity

(A) WT and *STING*^{Gt/Gt} mice bearing GL261-luc-gliomas in the brain received intratumoral injection of control solvent (closed circle or closed triangle, respectively) or c-di-GMP (open circle or open triangle, respectively) on day 10 following tumor inoculation (n=10/group). Survival was monitored. **p* < 0.05 based on Log-rank test. (B) On day 5 following the control (gray bars) or c-di-GMP (black bars) treatment, WT and *Sting*^{Gt/Gt} mice were sacrificed and their brains were harvested for qRT-PCR evaluation of *Ccl5* and *Cxcl10* expression levels. **p* < 0.05 based on Student's *t*-test. (C) At the same time as experiments in (B), total numbers of CD8⁺ (left panel) and CD4⁺ (right panel) T cells in BILs of WT and *Sting*^{Gt/Gt} mice were enumerated by flow cytometry. **p* < 0.05 based on Student's *t*-test. (D) IFN γ -producing CD8⁺ BILs were enumerated by flow cytometry. Each experiment was performed at least twice. **p* < 0.05 based on Student's *t*-test. (E) Mice bearing *Sleeping Beauty*-induced *de novo* gliomas received intracranial injection of c-di-GMP or control solvent (N=8/group). Percent changes in tumor volume from the day before treatment (baseline) to day +7 is shown for each mouse as a waterfall plot. Tumor volume was evaluated by bioluminescent imaging. **p* < 0.05 based on Fisher's exact test.

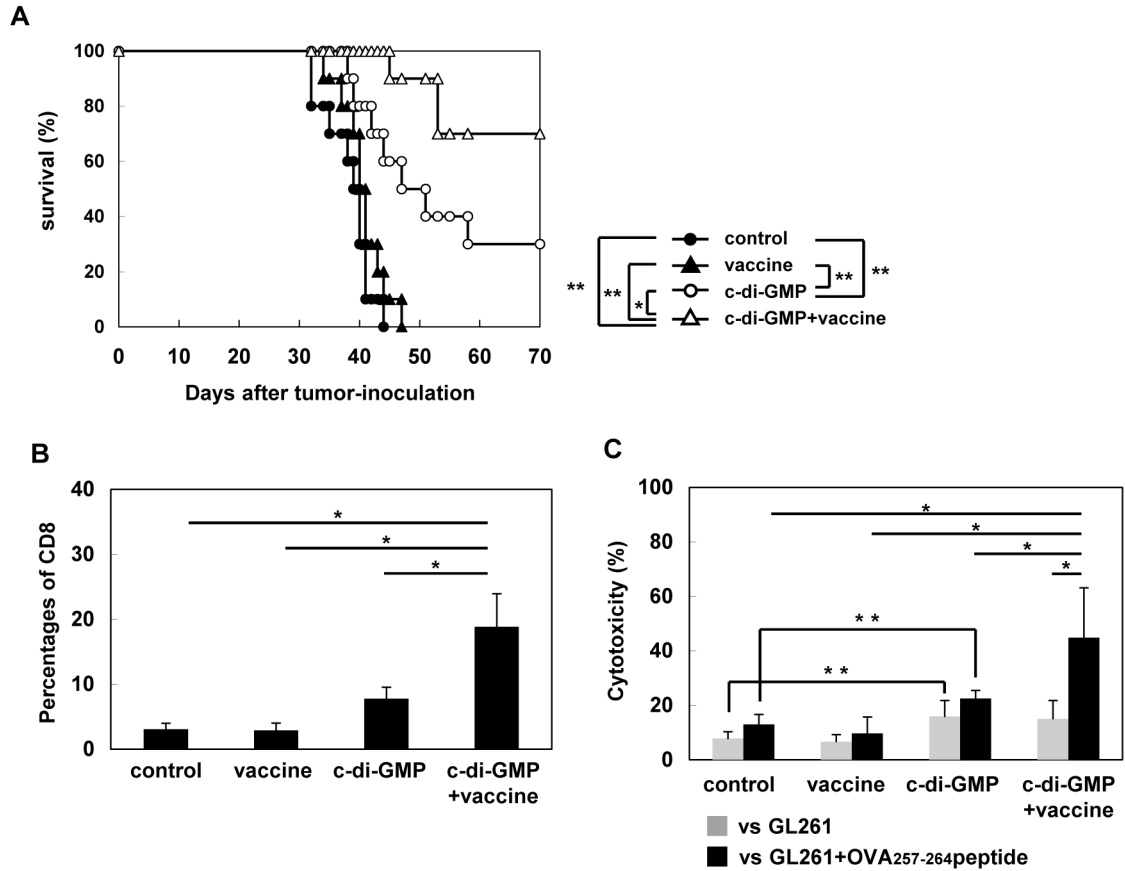


Figure 7. STING agonist enhances the efficacy of an OVA-targeted peripheral vaccine
 (A) Mice bearing Quad-GL261 glioma in the brain received with control solvent (N=10, closed circle), OVA peptide vaccination alone (N=10, closed triangle), c-di-GMP alone (N=10, open circle), or c-di-GMP with OVA peptide vaccination (N=10, open triangle) on day 14 following tumor inoculation. Survival was monitored. * $p < 0.05$, ** $p < 0.01$ based on Log-rank test. (B) CD8⁺ BILs were enumerated for each group by flow cytometry (5 mice/group). * $p < 0.05$ based on ANOVA test. (C) Cytotoxic activity of freshly isolated BILs against the vaccine-targeted OVA epitope was evaluated by ⁵¹Cr-release assay using control GL261 (gray bars) or OVA₂₅₇₋₂₆₄ peptide-pulsed GL261 cells (black bars) as target cells at E/T ratio 10 : 1 (5 mice/group). Each experiment was performed at least twice. * $p < 0.05$ based on ANOVA test. ** $p < 0.05$ based on Student's *t*-test.